



A Comparative Study of Unfolding Techniques for Gamma-Ray Spectra Obtained with NaI(Tl) Scintillation Detectors

Mwingereza J Kumwenda

Department of Physics, University of Dar es Salaam, P.O Box 35063, Dar es Salaam, Tanzania

E-mails: kmwingereza@yahoo.com, kmwingereza@udsm.ac.tz

Received 7 May 2024, Revised 2 Oct 2024, Accepted 20 Dec 2024, Published 31 Dec 2024

<https://dx.doi.org/10.4314/tjs.v50i5.8>

Abstract

Iterative unfolding methods are frequently used in acquiring true gamma-ray spectra from the measured spectra. However, the peak resolution of iterative unfolding methods especially, in Gold algorithm method is very challenging, especially in the case of scintillation detectors, where several instrumental artifacts and distortions interfere with the true spectral shape. Therefore, this paper presents a comparative study of the direct matrix inversion unfolding method (DMIUM) and iterative unfolding method with emphasis on the Gold algorithm method (GAM) in converting measured gamma-ray spectra of the NaI(Tl) scintillation detector into the true gamma-ray spectra. The Monte Carlo simulation based on the Geant4 software package was used to study the response function of the NaI(Tl) scintillation detector and for the formation of 200 by 200 response matrices. The results obtained from the number of the integrated photon counts of gamma-ray energies of 662 keV, 1173 keV, and 1333 keV respectively, for the DMIUM were 4, 91, and 93 times greater than in the original energy spectrum while for the GAM method were 3, 14, and 4 times greater than in the original energy spectrum. In conclusion, these results suggest that DMIUM is better in peak resolving ability than the GAM.

Keywords: DMIUM; Gamma-rays; GAM; NaI(Tl) detector; Integrated photon.

Introduction

Generally, the measured spectra in the physical experiments are usually distorted and transformed by different detector effects, such as finite resolution, limited acceptance, efficiency variations, and perturbations that may arise from the electronic devices. In order to reproduce the true photon spectrum from the measured spectra it is necessary to consider these effects (Benitez et al. 2008, Thuillier et al. 2022). To reproduce the detected spectra to get true spectra is very crucial in the effort towards extracting real spectra. The so-called spectra unfolding or deconvolution is one of the most powerful techniques currently used to obtain true energy spectra from the measured spectra which are of various types and different performance. The performance of unfolding

methods strongly depends on the process under analysis, thus, suggests the importance of comparing the unfolding methods to improve the accuracy of the interpretation of gamma-ray spectra obtained using scintillation detectors (Amade et al. 2020).

Various deconvolution methods have been proposed in nuclear and particle physics for accurate and precise of the measured gamma-ray spectra (Amade et al. 2020, Croston et al. 2018, Zech 2013). Some of the methods include the spectrum stripping, stochastic methods, Bayesian methods, linear regularisation, Maximum-likelihood fitting by expectation method (ML-EM), Maximum entropy method (MEM), Singular-value decomposition (SVD), Richardson-Lucy (RL), Gold unfolding method (GAM), and Direct matrix inversion unfolding method

(DMIUM) (Dombrowski 2023, Panontin et al. 2021, Meng and Ramsden 2000, Zech 2013, Pehlivanovic et al. 2012, Bouchet 1995). However, the methods mentioned in those studies were only tested on iterative methods except the direct matrix inversion unfolding method. Therefore, this study presents a comparison between the direct matrix inversion unfolding method and the Gold unfolding method as one of the iterative methods in order to quantitatively determine which of the two methods has a high ability to move the counts to the appropriate photo-peaks.

Materials and Methods
Experimental Setup

This study has made use of four identical cylindrical NaI(Tl) ORTEC 905-3 series detectors with crystals optically coupled to the PMT and encased in a light-tight aluminium case. The face of each detector had a diameter of about 5.08cm (2 inches by 2 inches) crystal size. The detectors are attached to pre-amplifiers to maintain the time constant of the pulse with a resolution of about 7% for Cs-137. They have a light decay time of 230 nanoseconds, which is translated to a voltage pulse of rise time of 0.5 microseconds. Each detector has 3 connectors

at its rear, high voltage (HV), Anode, and Dynode, which are damped by a 50-ohms resistor for this experiment (ORTEC 2015).

For convenience, the detectors were named with letter D1, D2, D3 and D4 then each detector was made to view the radioactive source. They arranged in such a way that each detector’s face was 5 cm away from the radioactive source as shown in Figure 1. All detectors were positively powered by a quad high-voltage power supply NIM module model RPH-012. Signals from each detector were passed through a linear split module, which had two outputs for each channel. From each channel, one signal was fed to the Analogue-to-Digital Converter (ADC; RPC-022 16ch CS) and the other signal was sent to the Leading-Edge Discriminating (LED) module. For each channel, one discriminated signal was fed into the coincidence unit, responsible for sending signals to the gate generator (KN1500) for triggering the event. The other discriminated signal from the same channel was delayed using a logic delay unit before being fed into the Time-to-Digital Converter (TDC; KC3781A). Trigger logic OR was used to provide event triggering condition (Kumwenda 2020). Figure 1 describes the complete data read out electronics that was used during experiment.

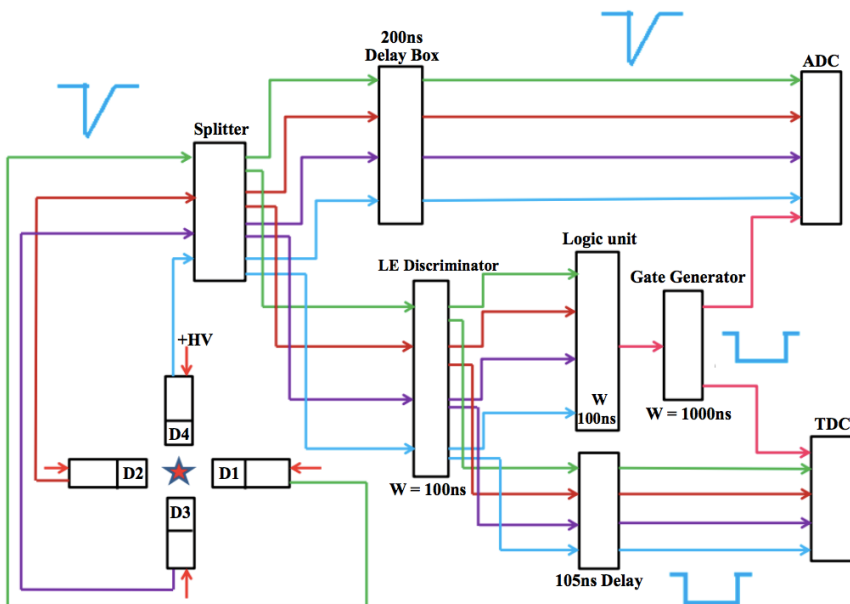


Figure 1: The electronic data readout circuit used during experiment (Kumwenda 2020).

Deconvolution Method

Direct Matrix Inversion Method

Normally the response functions are obtained from the response matrix. The measured spectrum $M(E)$ is generally calculated using equation (1).

$$M(E) = R(E, E_0)T(E_0) \quad (1)$$

where $T(E_0)$ represents the original or true energy distribution of the gamma rays emitted by the source and $R(E, E_0)$ is the matrix indicating the response function of the detector (Benitez et al. 2008, Thuillier et al. 2022).

The task is to obtain the true gamma-ray spectrum from the measured energy spectrum. Thus, the desired photon spectrum $T(E_0)$ was calculated from the matrix given by equation (2).

$$T(E_0) = R^{-1}(E, E_0)M(E) \quad (2)$$

where $R^{-1}(E, E_0)$ is the inverse of the response matrix. The pulse height from various mono-energetic gamma-ray spectra were obtained from Geant4 software package via Monte Carlo simulation using NaI(Tl) scintillation detector.

Simulation of Response Function

The Monte Carlo method based on the Geant4 software package codes was used to generate response matrix. The formation of the response matrix, might require over 100 spectra depending on the dimension of the problem, which is very time-consuming and tedious (Benitez et al. 2008). This study simulated 200 γ -ray's spectra ranging from 50 to 2040 keV at an interval of 10 keV as shown in Figure 2 in 2D.

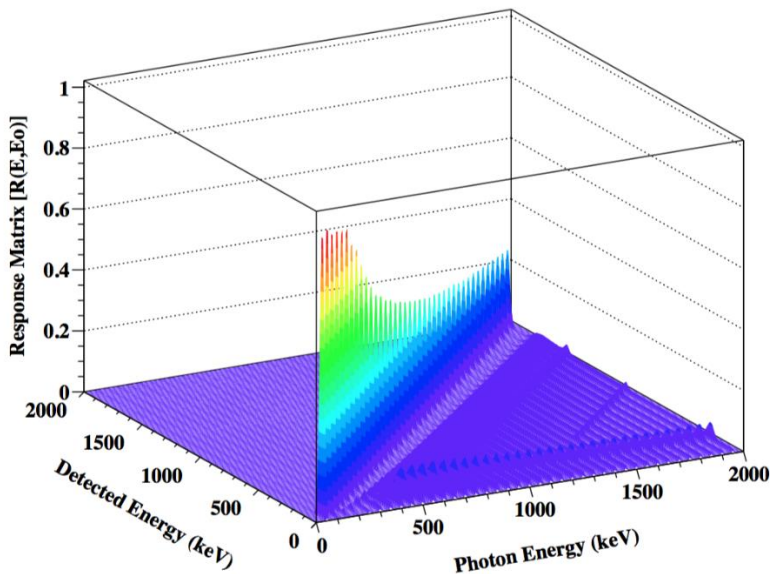


Figure 2: 2D simulated response function from various mono-energetic gamma rays using NaI(Tl) scintillation detector.

The z-axis of the 2D spectrum in Figure 2 shows the peak-to-total ratios that gives the diagonal elements of the response matrix. The peak at 200 keV is due to the Compton backscattering as a result of the random

direction of the gamma photons during simulation. The other peaks in the y-axis are single and double escape peaks when the gamma photons reach the threshold energy of 1.022 MeV (Kumwenda 2018).

To acquire meaningful results, the simulated response function must be obtained with the same conditions as experimental measurement setup. For the accuracy of the unfolding (equation 1), the response function $R(E, E_0)$ should have many energy points (Benitez et al. 2008). In the present work, the validity of

the simulated results was checked by comparing the experimental and simulated spectra (Figure 3). The comparison of the measured and simulated spectra was done using a radioactive standard gamma source of ^{137}Cs .

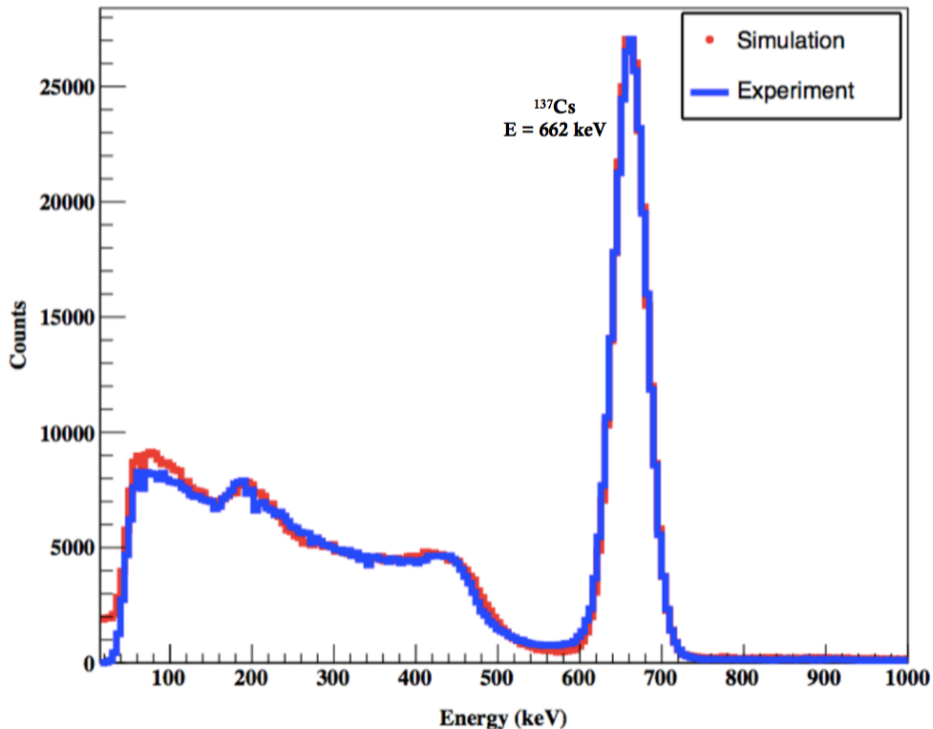


Figure 3: Comparison of experimental and simulated spectra (Kumwenda 2018).

Clearly, the results (Figure 3) show a good agreement between the simulated and measured spectra around the photo-peak region, with slight mismatch in the lower energy spectra below 200 keV. This discrepancy can be attributed to the effects of Compton backscattering that is also associated to the appearance of peaks in the simulated and measured profiles at around 200 keV. Note that the simulated spectra have lower counts between Compton edge and photo-peak that might be due to the broadening of a single Gaussian function.

Peak to Total Ratio

In a mono-energetic gamma-ray radiation pulse height spectrum, the Peak-to-Total (P/T)

ratio gives the number of counts in the total energy absorption to that contained in the whole spectrum. When a photon with energy E_0 is radiated there is a certain chance of being fully detected or partially detected. The probability that a photon of energy E_0 is fully detected with energy E is given by the response matrix $R(E, E_0)$. In order to obtain a response matrix $R(E, E_0)$ one needs to calculate the P/T ratio (Almaz and Cengiz 2007, Rahma and Cho 2010). To obtain the P/T ratio, the mono-energetic gamma spectrum peak was fitted to the

Gaussian functions, and the peak region was calculated by taking 1.96σ value that makes 95% confidence level for the peak region. The peak region boundary was established as $(\mu - 1.96\sigma, \mu + 1.96\sigma)$ and counts under

this region were divided by the total counts of the whole spectrum to obtain the P/T ratio that gives the diagonal elements of the response matrix (Figure 4).

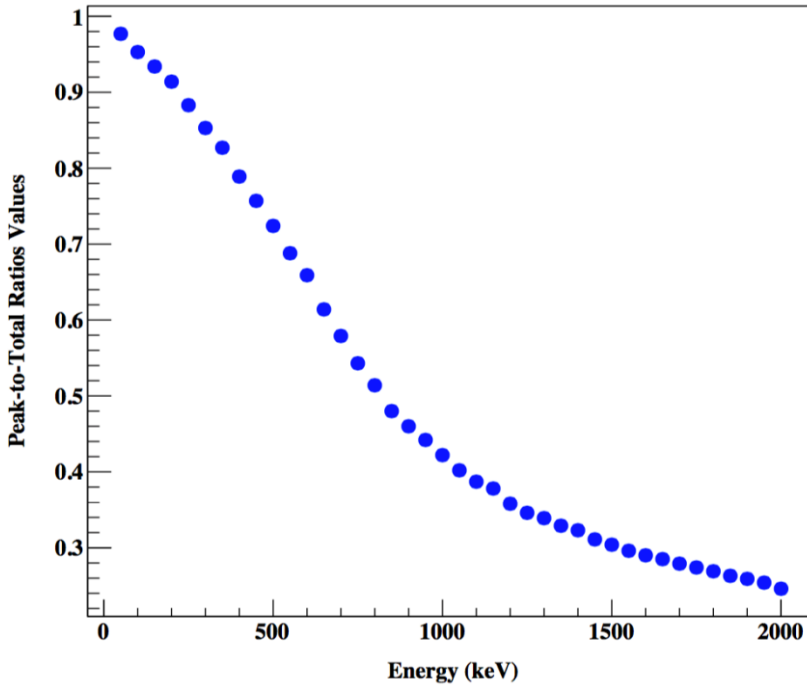


Figure 4: The P/T ratios curve showing the diagonal elements of the response matrix.

In order to fill in the remainder of $R(E, E_0)$ the P/T ratio for each photon energy E_0 was subtracted from the unity and the remainder was shared equally in the energy region between zero and Compton edge. This gives the maximum energy that can be absorbed due to Compton scattering is known as Compton Edge (E_c) and is given by equation (3).

$$E_c = \frac{2E_\gamma^2}{m_e c^2 + 2E_\gamma} \quad (3)$$

where m_e is the mass of an electron, c^2 is the speed of light, and E_γ is the photon energy.

Direct Matrix Inversion Method Procedures

Generally, unfolding methods are divided into two groups, namely, direct and iterative.

In the direct matrix inversion unfolding linear algorithm that was used in this study, the response matrices were arranged in rows and columns to form a M by M upper triangular response matrix. The obtained upper triangular matrices $M \times M$ were inverted using TMatrix class (*TMatrix::kInvert*) in a ROOT software of C++ programming language. To obtain vector $M(E)$, the measured spectrum was integrated in a 0.01 MeV energy interval. The matrices R^{-1} and column vector M were multiplied to obtain another column matrix T , which is the true gamma-ray spectrum of the detector. The acquired column matrix T was filled in the histogram and used to plot the true energy spectrum from the measured spectrum. The accuracy of the response matrix was checked

by multiplying R and R^{-1} . The results showed that all elements along the diagonal were unit while in the inverse matrix, all elements above the diagonal were negative numbers which are physically acceptable (Kumwenda 2020). When the measured spectrum vector M was multiplied by the inverted matrix R^{-1} due to photons of a given energy, the number of photons dropped entirely in the channel corresponding to the given energy in the true spectrum for the mono-energetic spectrum.

Gold Deconvolution Method

The Gold deconvolution algorithm is an iterative algorithm designed to obtain the best estimate of the true measured spectrum also called incident spectrum. The Gold deconvolution algorithm (equation 4) was proposed and used earlier by Morhac et al. (1997).

$$x^{(n+1)}(i) = \frac{y'(i)}{\sum_{m=0}^{M-1} A_{im} x^{(n)}(m)} x^{(n)}(i) \quad (4)$$

where $A = H^T H$, $y' = H^T y$ and $n = 0, 1, 2, \dots$ is the iteration steps, H is the matrix has a dimension $N \times M$, $x(i)$ is the input into the system and $y(i)$ is the output from the system. The solution of equation 4 is always positive when the input data are positive, which makes the algorithm suitable to use natural positive definite data known as spectroscopic data. At the

beginning of the iterations there is no prior information about the solution thus one sets;

$$x^{(0)} = [const, const, \dots, const] \quad (5)$$

From equation (5) it follows that the absolute value of $const$ is irrelevant. If all elements in the vector H , y are spectroscopic data the iteration converges to the least squares estimates in the constrained subspace of positive solutions (Morhac and Matousek 2011). The Gold deconvolution algorithm was implemented using C++ programming language and was tested using measured single and double peak energy sources of Cs-137 and Co-60, respectively.

Validation of Direct Matrix Inversion Unfolding Method

Multi-line energy spectra were employed to validate the unfolding method, using Ba-133. Ba-133 disintegrates by electron capture into $^{133}\text{Cs}^*$ excited levels of 437 keV (85.4%) and 383 keV (14.5%). It follows that excited Cs-133 decays to its stable ground state by emitting gamma rays of several energies (Be et al. 2008). As shown in Figure 5(a), the measured spectrum shows that the 81 keV line populates much more than the 356 keV energy line, accordingly the Ba-133 decay scheme the 356 keV energy line has a higher emission probability of 62.05% than the 81 keV (32.9%) energy line. Based on the direct matrix inversion unfolding method, the 356 keV gamma line of Ba-133 shows a higher emission probability as expected.

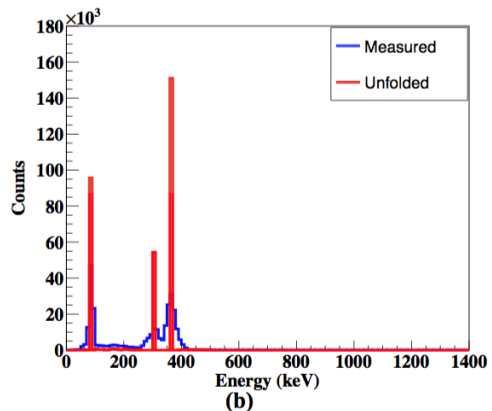
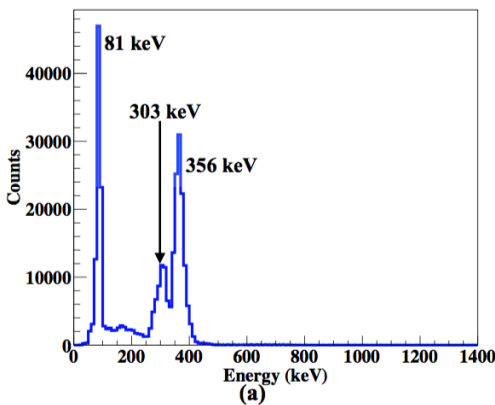


Figure 5: (a) Measured and (b) deconvoluted energy spectra of ^{133}Ba using the matrix method.

Results and Discussions

This study was modelled based on the experimental setup described previously using a single peak source (Cs-137), and double peak source of Co-60 in both unfolding methods. Co-60 decays to Ni-60 through beta minus emission. The decay is

initially to the nuclear-excited state of Ni-60 from which it emits either one or two gamma rays to reach a ground state of the Ni-60 isotope (Be et al. 2008). The creation of Ni-60 by the beta minus emission of Co-60 is described by the decay scheme in Figure 6.

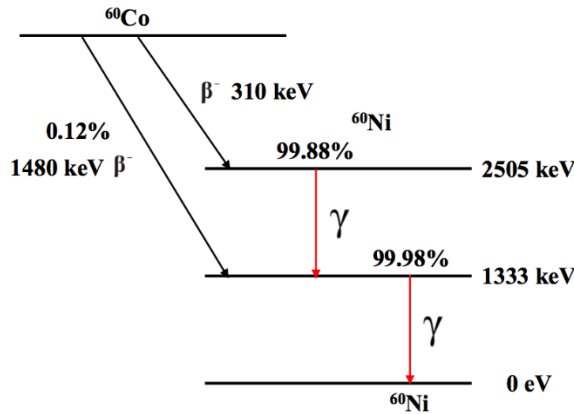


Figure 6: The decay scheme of Co-60, showing the two gamma lines.

From the decay scheme (Figure 6), it was observed that Co-60 has two gamma lines with almost the same probability of emission. However, as shown in Figure 7, the 1333 keV line was observed to populate much less than the lower line of 1172 keV. As expected the

deconvolution for Co-60 decay resulted in the almost same probability of emission. This is shown in Figures 8 and 9 for the direct matrix inversion method and the Gold algorithm method respectively.

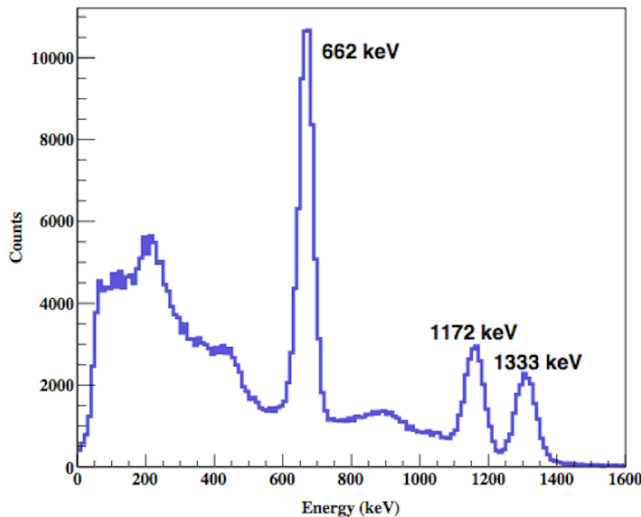


Figure 7: Measured energy peaks of 662 keV for Cs-137 and 1172 keV, 1333 keV for Co-60.

Figure 8 shows the results of unfolded energy spectra of Co-60 using the direct matrix inversion method while Figure 9 shows the results of unfolded energy spectra of Co-60 using the Gold algorithm method.

In comparison, both methods decompose the spectrum practically to a delta-like function, which was expected however there are some variations in the Gold algorithm method caused by some oscillations in the iterations.

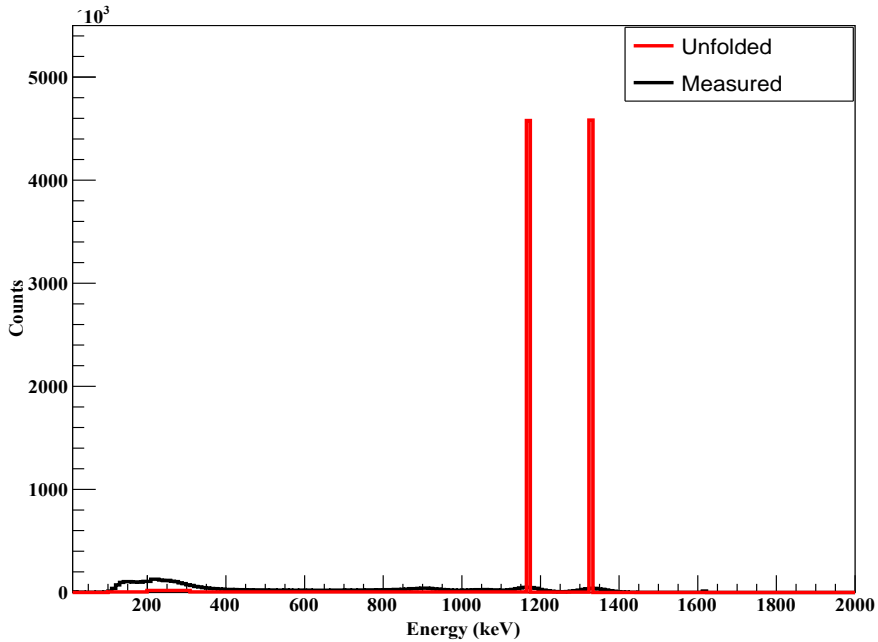


Figure 8: Unfolded energy spectra of Co-60 (red histogram) using direct matrix inversion unfolding method.

The results in Figures 9 (a) and (b) reveal small and overlapped peaks (multiples) caused by some oscillations in the deconvoluted spectra of 10 and 100 iterations respectively. These small peaks were observed to completely disappear from the deconvoluted spectra as in 9 (c-d) as the number of iterations increased. This result implies that the better performance of the Gold unfolding method depends on the large number of iterations, this is contrary to the direct matrix inversion method where there is no dependence of the iterations.

In comparison of the two isotopic sources (Cs-137 and Co-60) spectra, the plots revealed that the Compton scattering region and the backscatter peak (below the photo-

peaks) counts were successfully moved to the photo-peaks as shown in Figures 8, 9, 10 (b), and 11. These results suggest that the energy resolution for each of the photo-peaks unfolded was improved more than in the original (measured) energy spectrum. Figures 11 (a-d) show the unfolded energy spectra of Cs-137 using the Gold unfolding algorithm method. The implication of Figures 11 (a-d) is that, with the increasing number of iterations the width of the peak gets narrow resulting in better smearing of the measured spectra. This implies that the performance of the Gold unfolding method depends on the number of iterations.

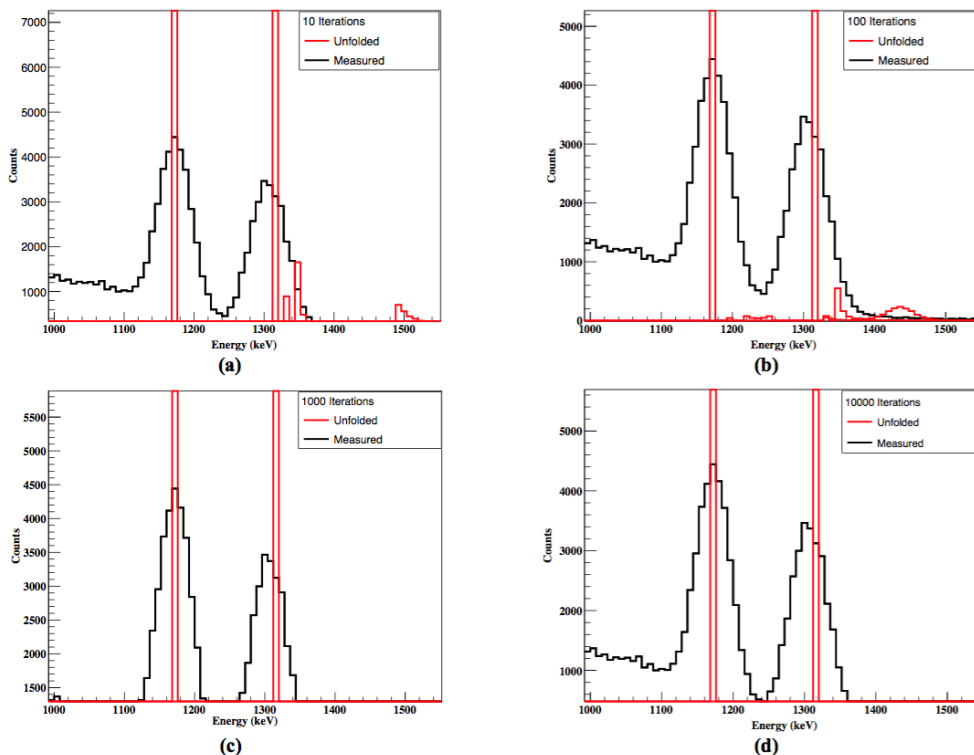


Figure 9: Deconvoluted energy spectra of Co-60 (red histogram) using Gold algorithm method (a) 10 iterations (b) 100 iterations (c) 1000 iterations and (d) 10000 iterations.

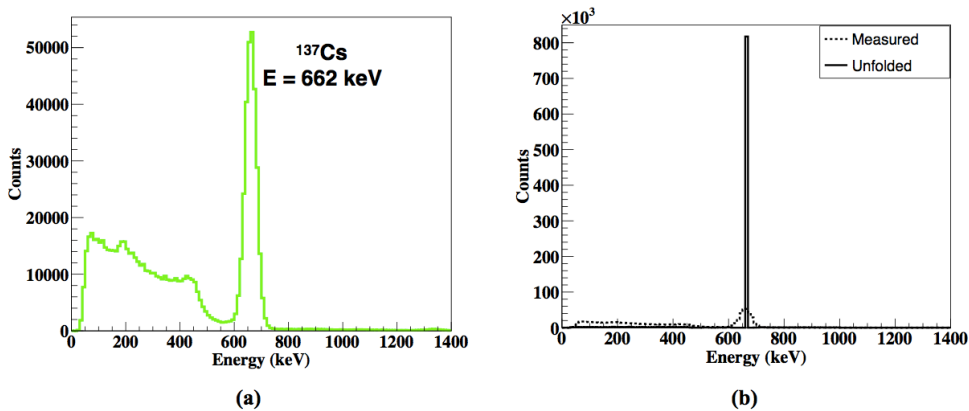


Figure 10: (a) Measured energy spectrum of ^{137}Cs (green histogram) and (b) The deconvoluted (black histogram) using matrix inversion unfolding method.

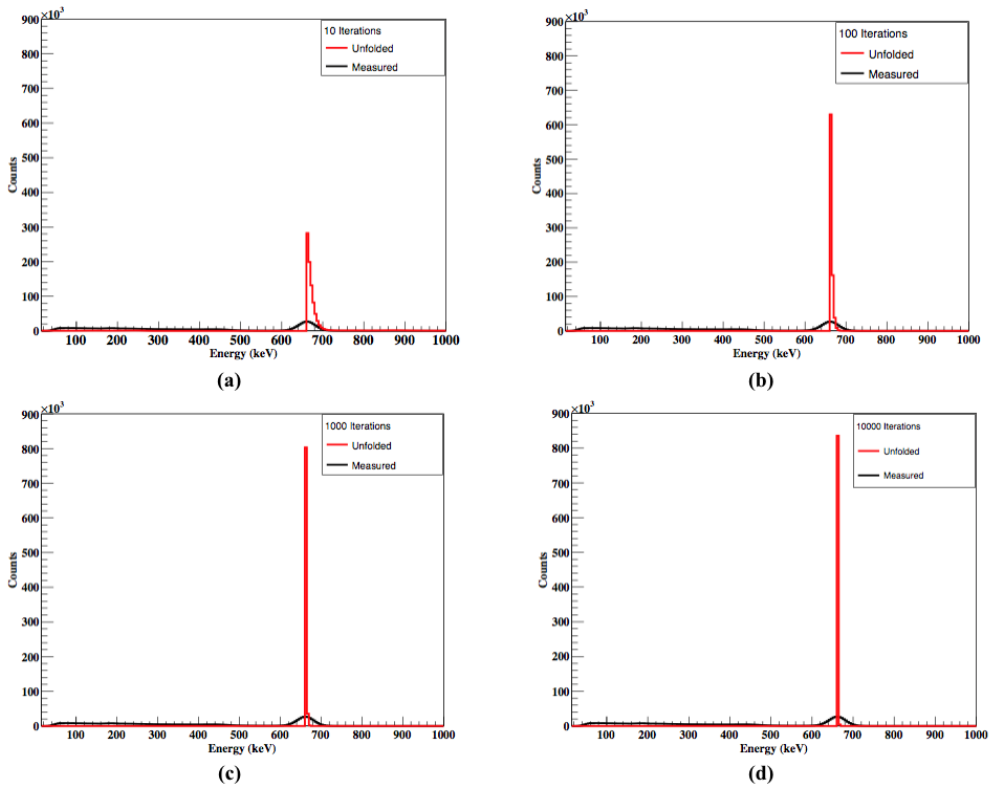


Figure 11: Unfolded energy spectra of Cs-137 (red histogram) using Gold algorithm method (a) 10 iterations (b) 100 iterations (c) 1000 iterations and (d) 10000 iterations.

Furthermore, the number of integrated photon events for two calibration radioactive gamma-ray sources was calculated to quantify the efficiency of both methods in moving the photon counts to their appropriate Gaussian shape photo-peaks. The integrated photon events taken with two calibration sources explicitly Cs-137 and Co-60 for gamma-ray energies of 662 keV, 1173 keV, and 1333 keV respectively, were increased from (to) 270688(1287636), 20816(1912642), and 16469(1543061) after application of the direct matrix unfolding method as shown in Figure 12. For the Gold algorithm method, the integrated photon events were also increased from (to) 270688(839813), 20816(297974), and 16469(72376). The results revealed that the number of the integrated photon counts (for the direct

matrix unfolding method) of gamma-ray energies of 662 keV, 1173 keV, and 1333 keV respectively, were 4, 91, and 93 times greater than in the original energy spectrum while for the Gold algorithm method were 3, 14, and 4 times greater than in the original energy spectrum. The results reveal generally that the direct matrix inversion unfolding method gives a better peak resolution than the Gold algorithm method. In comparison, the results presented in this paper are in good agreement with earlier studies that showed when the direct matrix inversion unfolding method was applied the number of integrated photon counts increased in the photo-peaks resulting to improvement of the detector energy resolution (Amade et al. 2020, Rahma and Cho 2010).

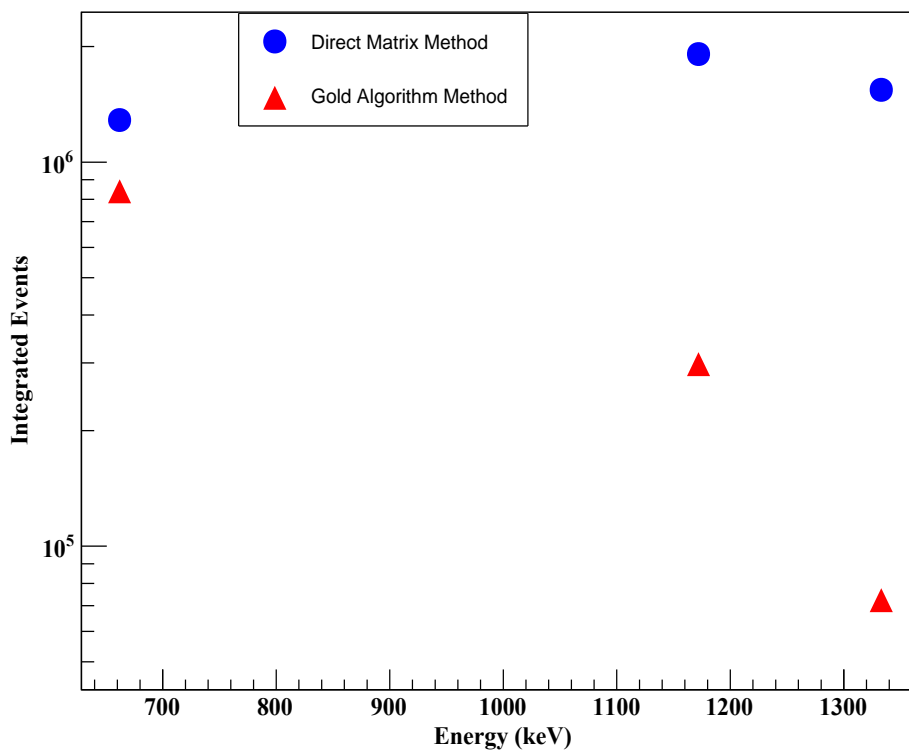


Figure 12: Integrated photon events obtained from direct matrix inversion unfolding method (blue) and Gold algorithm methods (red).

Conclusions

This paper presents the comparative study of the direct matrix inversion unfolding method and Gold algorithm unfolding method and conversion of the measured gamma-ray spectrum of the NaI(Tl) scintillation detector into the photo-peak by restoring counts from the Compton backscattering and Compton continuum into their corresponding photo-peaks. The Monte Carlo simulation based on the Geant4 software package was used to study the response function of the NaI(Tl) scintillation detector and formation of the 200 by 200 response matrices. The numbers of the integrated photon count were obtained from the energy spectra using two calibration sources of Cs-137 (662 keV) and Co-60 (1173 keV, 1333 keV). The Compton backscattering and Compton continuum counts were significantly transferred into the corresponding photo-peaks and consequently, the energy resolution was improved. The

results from both unfolding methods revealed that the spectrum retains its original shape of a delta-like function. The results suggests further that the direct matrix inversion unfolding algorithm gives a more precise identification of the spectrum and removal of electronic fluctuations in the measured spectrum than using the Gold algorithm unfolding method. Therefore, the direct matrix inversion unfolding method is better in peak resolving ability than the Gold algorithm method.

Declaration of Competing Interest

The author declares that there is no conflict of interest regarding this work.

Acknowledgements

The author would like to gratefully acknowledge support from the National Research Foundation of Korea and the University of Dar es Salaam, Tanzania, as well as Professor Ahn, and Dr. Lee of the Korea University.

References

- Amade NS, Bettelli M, Zambelli N, Zanettini S, Benassi G and Zappettini A 2020 Gamma-ray spectral unfolding of CdZnTe-based detector using a genetic algorithm. *Sensors*. 20, 7316.
- Almaz E and Cengiz A 2007 Deconvolution of continuous internal bremsstrahlung spectra of ^{32}P , ^{85}Kr and ^{143}Pr . *X-Ray Spectrometry* 36: 419-423.
- Be MM, Chiste V, Dulieu C, Browne E, Chechev V, Kuzmenko, HR, Nichols A, Schonfeld E, and Dersch R 2008 Table of radionuclides, vol. 4. Monographie BIPM-5.
- Benitez JY, Noland JD, Leitner D, Lyneis C, Todd DS and Verboncoeur J 2008 High energy component of X-ray spectra in ECR ion sources. *In Proc. ECRIS'08*, Chicago, IL, USA, paper MOPO-08: 77-84.
- Bouchet L 1995 A comparative study of deconvolution methods for gamma-ray spectra. *Astron. Astrophys. Suppl. Ser.* 113, 167-183.
- Croston JH, Arnaud M, Pointecouteau E and Pratt GW 2018 An improved deprojection and PSF-deconvolution technique for galaxy-cluster X-ray surface-brightness profiles. *Astronom. Astrophys* 459(3): 1007-1019
- Dombrowski H 2023 GRAVEL unfolding of gamma-ray spectra of CeBr3 detectors and related uncertainties. *J. Instrument.* 18(07): P07005.
- Kumwenda MJ 2018 *Measurements of bremsstrahlung photons in 28 GHz electron cyclotron resonance plasma*. Ph D thesis, Korea University.
- Kumwenda MJ 2020 Deconvolution of mono-energetic and multi-lines gamma-ray spectra obtained with NaI(Tl) scintillation detectors using direct matrix inversion method. *Tanzania J. Eng. Technol.* 39(2):104-115.
- Meng LJ and Ramsden D 2000 An inter-comparison of three spectra-deconvolution algorithms for Gamma-ray spectroscopy. *IEEE Trans. Nucl. Sci.* 47(4), 1329-1336.
- Morhac M and Matousek V 2011 High-resolution boosted deconvolution of spectroscopic data. *J. Comput. Appl. Math.* 235: 1629-1640.
- Morhac M, Kliman J, Matousek V, Veselsky M and Turzo I 1997 Efficient one and two dimensional Gold deconvolution and its application to gamma-ray spectra decomposition. *Nucl. Instrum. Methods Phys. Res. A.* 401 (2-3), 385-408.
- Panontin E, Molin AD, Nocente M, Groci G, Eriksson J, Giacomelli L, Gorini G, Iliasova M, Khilkevitch E, Muraro A, Rigamonti D, Salewski M, Scionti J, Shevelev A and Tardocchi M 2021 Comparison of unfolding methods for the inference of runaway electron energy distribution from gamma-ray spectroscopic measurements. *J. Instrum.* 16 C12005.
- Pehlivanovic B, Avdic S, Marinkovic P, Pozzi SA and Flaska M 2012 Comparison of unfolding approaches for mono-energetic and continuous fast-neutron energy spectra. *Radiat. Measure.* 49: 109-114. Radiation Measurements. <https://doi.org/10.1016/j.radmeas.2012.12.008>.
- Rahma MS, and Cho G 2010 Unfolding low-energy gamma-ray spectrum obtained with NaI(Tl) in air using matrix inversion method. *J. Sci. Res.* 2 (2), 221-226.
- Thuillier T, Benitez J, Biri S, and Racz R 2022 X-ray Diagnostics of ECR ion sources techniques, results, and challenges. *Rev. Sci. Instrum.* 93: 021102.
- Zech G 2013 Iterative unfolding with the Richardson-Lucy algorithm. *Nucl. Instrum. Methods Phys. Res. A.* 716, 1-9.